JMEPEG (2005) 14:647-653
DOI: 10.1361/105994905X64558

1059-9495/$19.00

Microstructural Alterations Associated With Friction Drilling of Steel, Aluminum, and Titanium

Scott F. Miller, Peter J. Blau, and Albert J. Shih

(Submitted May 26, 2005)

Friction drilling, also called thermal drilling, is a novel sheet metal hole-making process. The process involves forcing a rotating, pointed tool through a sheet metal workpiece. The frictional heating at the interface between the tool and workpiece enables the softening, deformation, and displacement of work-material and creates a bushing surrounding the hole without generating chip or waste material. The bushing can be threaded and provides the structural support for joining devices to the sheet metal. The research characterizes the microstructures and indentation hardness changes in the friction drilling of carbon steel, alloy steel, aluminum, and titanium. It is shown that materials with different compositions and thermal properties affect the selection of friction drilling process parameters, the surface morphology of the bore, and the development of a highly deformed layer adjacent to the bore surface.

Keywords machining, metallography, optical microscopy, tribology

1. Introduction

Friction drilling is a nontraditional hole-making method that uses the heat generated from friction between a rotating conical tool and the workpiece to soften and penetrate the work-material and generate a hole (Ref 1, 2). Friction drilling is also called thermal drilling, flow drilling, form drilling, or friction stir drilling. It forms a bushing in situ from the sheet metal workpiece and is a clean, chipless process. High temperature and strain in friction drilling change material properties and microstructures. These consequences, although often unwanted in machining, are both unavoidable and important to the quality of friction drilled holes. The development of microstructures is affected by the material flow and heating that occurs during friction drilling.

Unlike traditional drilling that uses cutting fluid to reduce the friction and heat generation, friction drilling is a dry process. Occasionally, a small amount of lubricant is used to avoid material transfer or adhering of the work-material to the tool surface. Also, unlike the traditional drilling, there is no chip or waste of material in friction drilling. All work-material from the hole contributes to form the bushing and boss. Friction drilling is a clean and environmentally benign manufacturing process.

The four steps in friction drilling and the tool geometry are schematically shown in Fig. 1. First, the tip of the conical tool approaches and penetrates the workpiece, as shown in Fig. 1(a). The friction force on the contact surface generates heat that softens the work-material. As the tool enters the workpiece (Fig. 1b), it pushes the softened work-material sideward and pierces through the workpiece. Having penetrated the workpiece, as shown in Fig. 1(c), the tool moves further forward to form the bushing using the cylindrical section of the tool. The shoulder of the tool may contact the workpiece to trim or collar the extruded burr on the boss (Fig. 1d). Finally, the tool retracts and leaves a hole with a bushing on the workpiece. The thickness of the bushing is usually two to three times that of the original workpiece. The thicker section in the hole can be threaded to provide better support for joining devices to the sheet metal workpiece.

Numerous researchers have studied friction drilling (Ref 1-6). Several technical papers and articles have been written regarding friction drilling. France et al. (Ref 7-9) investigated the strength characteristics of friction drilled holes in metal tubing. Overy (Ref 10) and Bak (Ref 11) discussed the design aspect of the friction drilled holes. Kerkhofs et al. (Ref 12) studied the performance of coated friction drilling tools. These publications describe friction drilling tools, equipment needed, and evaluate performance issues of the tool and bushing created. A more comprehensive analysis of experimentally measured thrust force, torque, temperature, and development of a semiempirical force model for friction drilling are presented in Ref 13. However, no study has been conducted to investigate the changes to microstructures and material properties of the work-material, which is subjected to the large deformation and high temperature in friction drilling.

The present work focuses on the microstructural alterations and subsurface microindentation hardness changes produced as a result of the friction drilling process of AISI 1020 and 4130 steel, Al 5052, and commercially pure (CP) titanium. Effects of temperature and plastic strain in friction drilling are investigated.

2. Experimental Setup

2.1 Materials

The tool used was a proprietary Co-bonded WC product supplied by Formdrill (Libertyville, IL). The tool geometry is important to the shape of the bushing and process performance.

Scott F. Miller and **Albert J. Shih,** Department of Mechanical Engineering, University of Michigan, Ann Arbor, MI 48109-2125; and **Peter J. Blau,** Metals and Ceramics Division, Oak Ridge National Laboratory, P.O. Box 2008 – M/S 6063, Oak Ridge, TN 37831-6063. Contact e-mail: blaupj@ornl.gov.

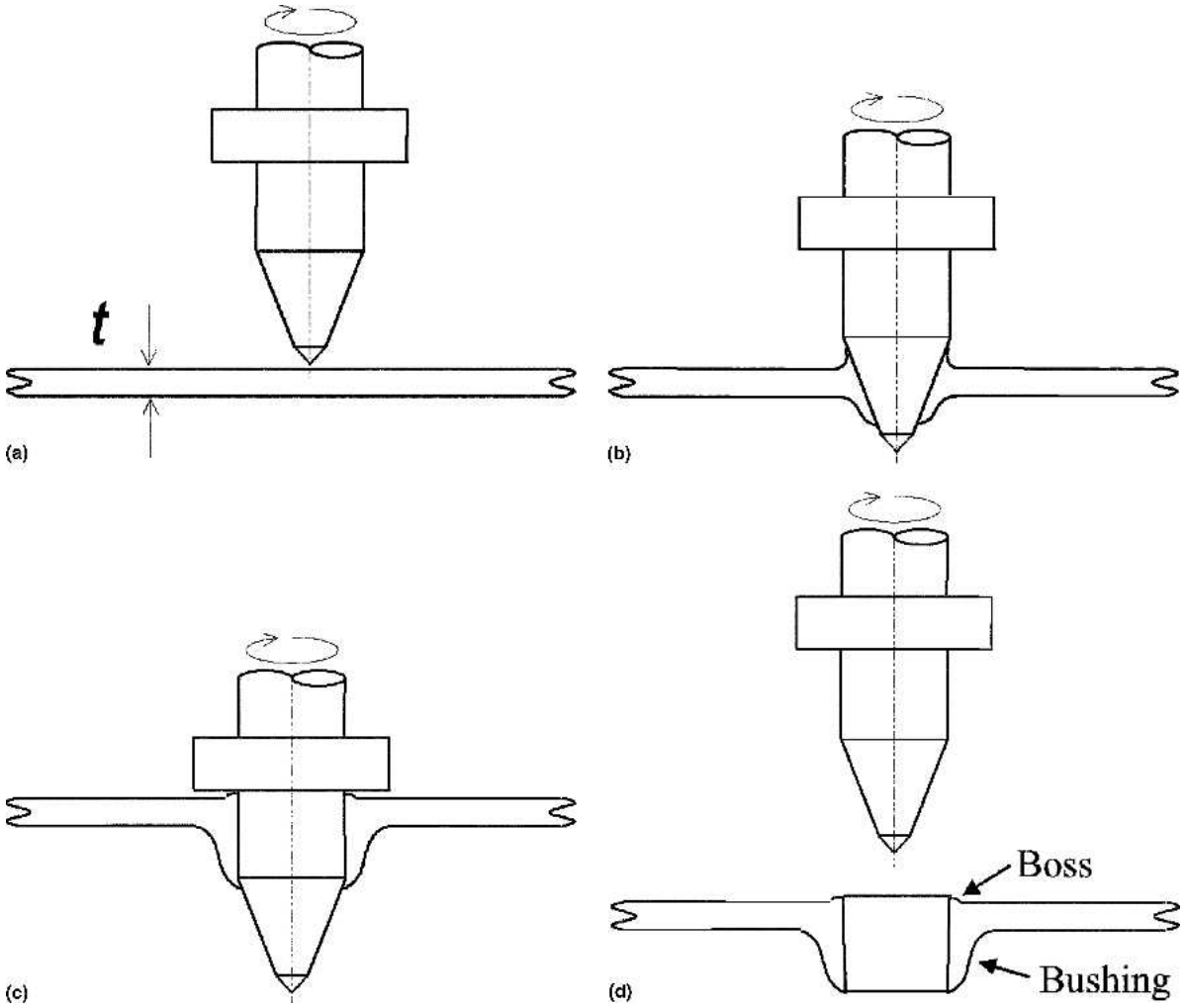

Fig. 1 Illustration of stages in the friction drilling process: (a) start of contact, (b) tool penetrating, (c) bushing and boss forming, and (d) drilled hole

Table 1 Materials used in friction drilling studies

Material	Sheet thickness, mm	Knoop hardness (0.245 N load), GPa	Thermal conductivity(a), W/m · K	Heat capacity(b), J/kg · K	Density(c), kg/m^3
AISI 1020 steel	1.56	1.67	50.2	481	7,850
AISI 4130 steel	1.43	3.11	41.2	477	7,845(d)
Al 5052	1.62	0.60	138	880	2,657
Commercially pure Ti	1.59	1.46	16.4	519	4,540
WC/Co (tool)	…	18.4	84	240	15,000

(a) Values at room temperature from Ref 14; (b) Values at room temperature from Ref 15; (c) Values at room temperature from Ref. 16; (d) Values at room temperature from Ref 17

The friction drill used in this experiment has an outer diameter of 5.3 mm and the height of the conical region is 6.35 mm.

The four workpiece materials chosen were AISI 4130 and 1020 steel, aluminum alloy 5052-H32, and Grade 2 CP titanium. The thickness and mechanical and thermal properties of the work-materials used in this study are listed in Table 1. Table 2 summarizes the chemical composition of the steel and aluminum alloy work-materials.

2.2 Drilling Parameters

A Vetrax vertical mill (Libertyville, IL) was used for friction drilling tests. The thrust force could be more accurately maintained constant with manual operation than using a constant feed rate in a conventional CNC machine, which generates high peak force as described by Miller et al. (Ref 13). This method helped to minimize denting the sheet metal workpiece

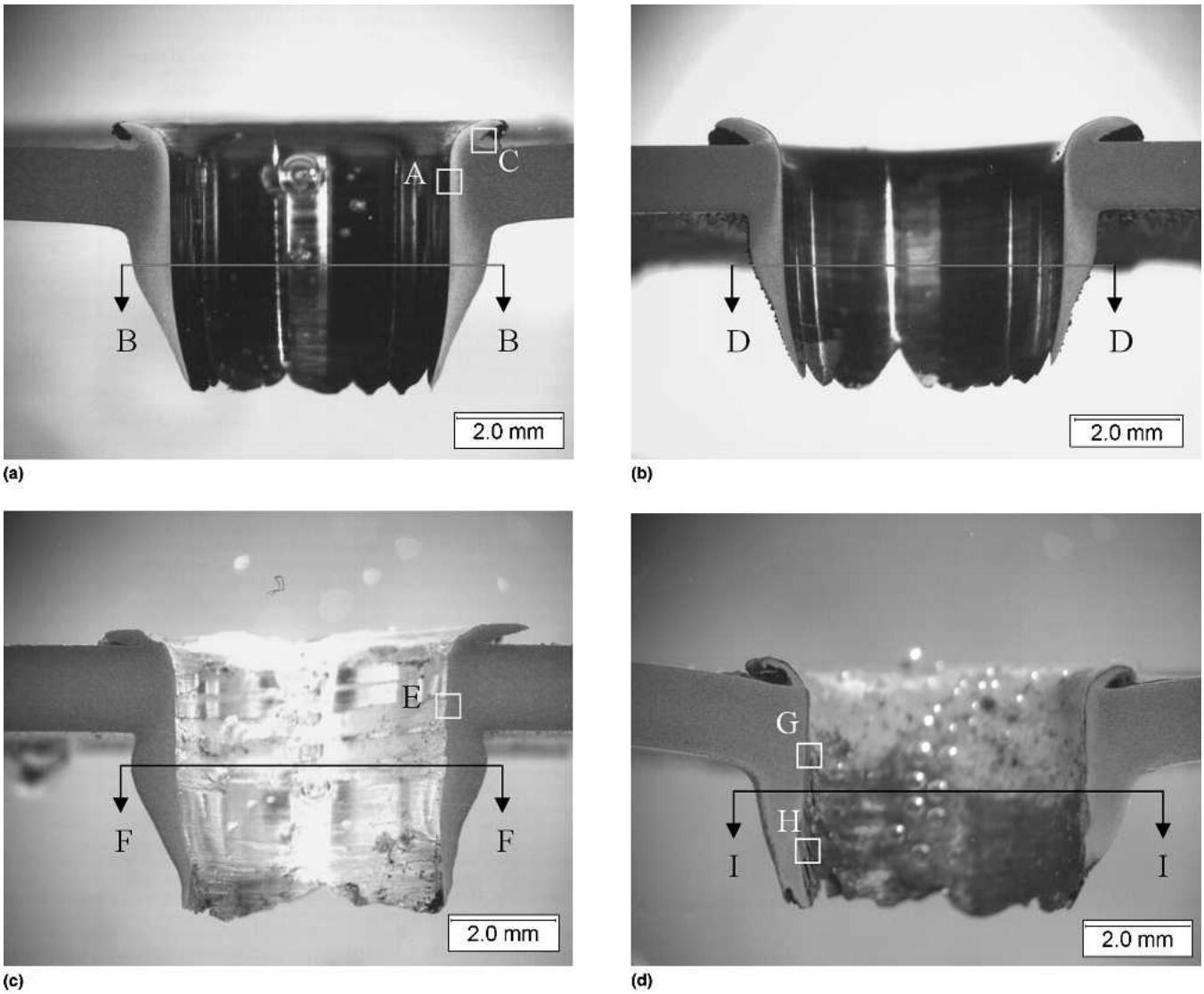

Fig. 2 Cross sections of friction-drilled holes in (a) AISI 1020 steel, (b) AISI 4130 steel, (c) Al 5052, and (d) CP Ti. Bubbles in (a), (c), and (d) are the mounting medium and should be ignored.

Table 2 Composition of as-received sheet metal by wt.% (Ref 18)

Element	AISI 1020 steel	AISI 4130 steel	Al 5052-H32
Al			95.7-97.7
C	0.17-0.23	0.28-0.33	
Cr		0.8-1.1	0.15-0.35
Cu			Max 0.1
Fe	99.08-99.53	97.3-98.22	Max 0.4
Mg			2.2-2.8
Mn	0.3-0.6	0.4-0.6	Max 0.1
Si		0.15-0.35	Max 0.25
Zn			Max 0.1
P	Max 0.04	Max 0.035	
S	Max 0.05	Max 0.04	
Mo		0.15-0.25	

and to improve the bushing quality. The fixturing and instrumentation for drilling is the same as in Miller et al. (Ref 13).

The spindle speeds used for sheet material of AISI 4130 steel, 1020 steel, CP Ti, and Al 5052 were 2800, 2800, 1000, and 3600 rpm, respectively. These were determined experimentally to enable the penetration and forming of the hole. For titanium, with low thermal conductivity, most of the frictional heat is retained in the tool-workpiece interface. The effect of frictional heating is relatively prominent. This causes excessive temperatures in the workpiece and results in undesired material damage and improper bushing formation. For the aluminum alloy, the thermal conductivity is high. A large portion of the frictional heat is transferred into the workpiece and the effect of friction heating is relatively small. Low temperature causes insufficient increase in ductility and softening, resulting in high thrust force, denting of the workpiece, and improper bushing formation. These effects dictated the selection of low and high spindle speed for titanium and aluminum, respectively. These settings, while satisfactory for the present studies, do not necessarily represent the optimal drilling conditions that might be used in a production environment.

A specimen of each workpiece material was prepared for examination. A friction drilled hole was cut from the workpiece sheet metal. Each was mounted in a metallographic mount by epoxy potting, then rough ground to the hole cross-section, and then polished with progressively finer diamond

compounds. This preparation facilitated examination by optical microscopy and hardness testing by a Buehler microhardness tester. The Knoop indenter under 0.245 N load was used for microhardness indentation tests. The elongated impressions of the Knoop hardness test enables closer spacing within the deformed regions. After optical microscopy and hardness testing, the specimens were chemically etched for microstructural observation. Chemical etchants were applied to reveal the grain boundary and observe the large plastic deformation of work-material, particularly the surface layer, on friction drilled holes (Ref 19).

3. Microstructure Observations and Discussion

Figures 2(a)-2(d) show low magnification, optical views of the polished cross sections of the four work-materials. Differences in the material displacement are evident as is the shape of bushing, bore surface quality, and denting of the workpiece. Table 3 summarizes macroscopic measurements of holes and shape of bushings that were produced by friction drilling. The steels had relatively smooth bore finishes, as shown in Fig. 2(a) and 2(b). However, the aluminum (Fig. 2c) and titanium (Fig. 2d) holes show severe tearing and scoring on the hole surface. The light-colored deposit in the titanium hole is residue from the drilling lubricant. Bubbles apparent in Fig. 2 exist in the mounting epoxy and are not relevant in the cross-section samples. The photomicrographs that follow show planes of polish parallel to the cross-sectional view as shown in Fig. 2 or from a top view parallel to the original sheet. Since nonferrous work-materials responded differently to friction drilling than the steels, these will be discussed in separate sections.

3.1 AISI 1020 and 4130 steels

Friction drilled holes in AISI 1020 and 4130 steel were relatively uniform in shape and exhibited a smooth bore surface finish. No material transfer was noticed for friction drilling of these ductile materials. Figure 3(a) shows box A in Fig. 2(a), the subsurface microstructure adjacent to the hole bore in AISI 1020 steel. A region of relatively fine-grained, equiaxed grains extend approximately 60 μm radially from the hole surface, marked by J. These grains appear to be 1 μm or less in diameter. Inside this subsurface region, a larger region of elongated grains is visible.

Figure 3(b) shows a hole in AISI 1020 steel but with the plane of polish parallel to the plane of the sheet in the bushing, as shown by line B-B in Fig. 2(a). It shows the similar microstructurally deformed area, marked by K, and a surface texture that suggests the tool rotational direction (the surface was frictionally sheared from the left to the right in the photomicrograph).

Knoop microindentation (the indentation load was 0.245 N) subsurface hardness profiles comparing the AISI 1020 with that of AISI 4130 steel are shown in Fig. 4. The zone of high hardness caused by the severe plastic deformation for AISI 1020 appears to extend 120 μm below the surface, while AISI 4130 drops off more steeply at about 60 μm below the surface. The AISI 4130, as expected, has higher hardness values. Hardening also occurred on the upset portion of the boss region, indicated as box C in Fig. 2(a). Figure 5 shows the microstructural texturing in this zone on AISI 1020 steel. The indentation hardness of this upset region was 3.01 GPa, but that of the drawn out tip at the bottom end of the hole was less, about 2.29 GPa. Both hardness values in the boss region are higher than that of the sheet well away from the hole, about 1.46 GPa.

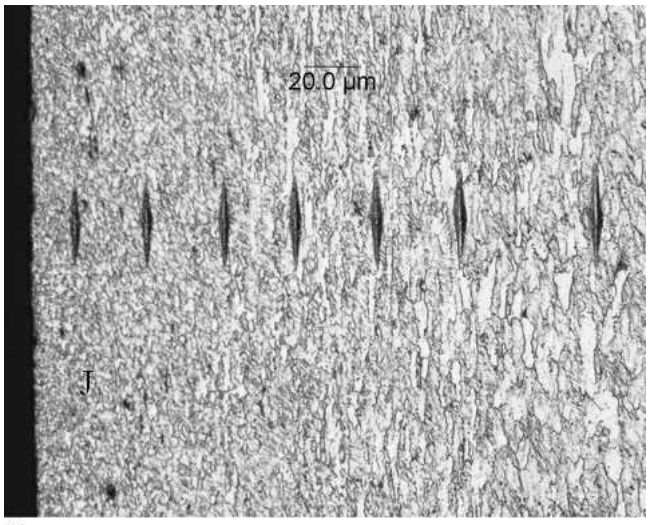

(a)

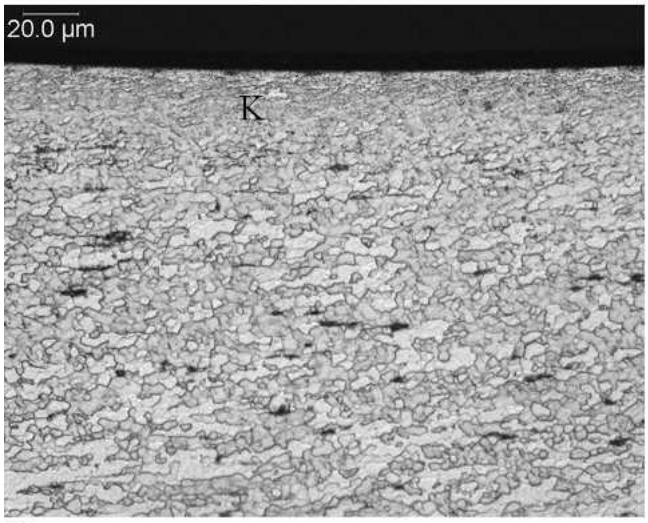

(b)

Fig. 3 (a) Close-up view of box A in Fig. 2(a), shear deformation zone adjacent to the cylindrical portion of the hole in AISI 1020 steel showing a row of Knoop hardness impressions (etched in 2% nital) and (b) cross-sectional view of line B-B in Fig. 2(a) [same etchant as in (a)]

Table 3 Macroscopic measurements of hole characteristics

Material	Hole diameter, mm	Average boss extruded height above the sheet, mm	Average bushing height below the sheet, mm	Diameter of the base of the bushing, mm
AISI 1020 steel	5.22	0.38	2.96	4.83
AISI 4130 steel	5.28	0.51	4.12	5.28
Al 5052	5.24	0.42	4.14	5.30
CP Ti	5.19	0.32	2.83	4.87

The microstructure of the AISI 4130 steel adjacent to the hole, marked as line D-D in Fig. 2(b), is shown in Fig. 6. Compared with the same region of AISI 1020 in Fig. 3(b), the highly-strained, white-etching surface layers and overlapping

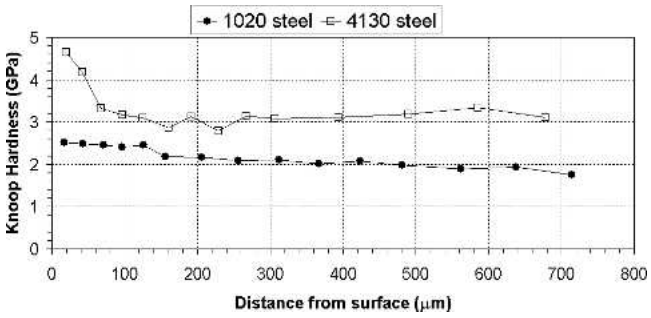

Fig. 4 Microindentation hardness profiles of subsurface in friction drilled AISI 1020 and 4130 steel workpiece (0.245 N force used)

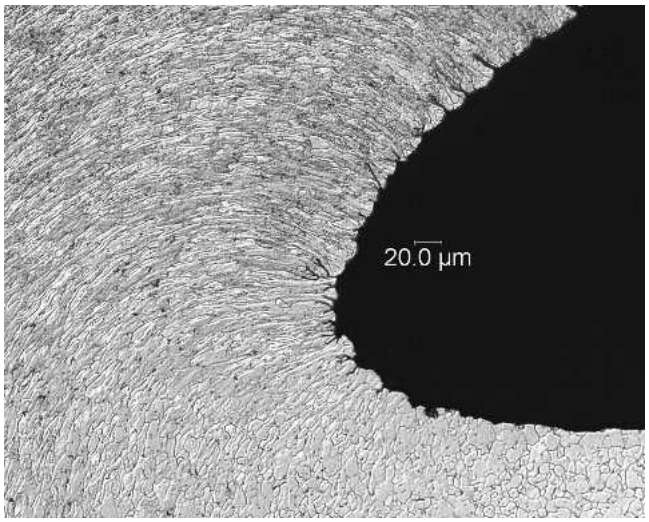

Fig. 5 Close-up of box C in the boss region of AISI 1020 in Fig. 2(a) showing extreme plastic flow in the region underneath the lip of upset material at the tool-entry side

surface texture are evident in the bore of the drilled hole of AISI 4130 steel. Surface tractions and localized shear strains apparently produced a fine series of parallel lamellae. The serrated appearance of the cross section is suggestive of ductile tearing.

3.2 Al 5052

Damage to the interior surface of the friction-drilled hole in Al 5052 sheet is evident in Fig. 7. Severe scoring and plastic deformation with surface delamination are present. Figure 8(a), marked as box E on the cross section in Fig. 2(c), exhibits thin platelets of aluminum that were removed, leaving some regions with microcracking below the deformed layers. The tendency of aluminum adhering to metalworking and machining tools is commonly known (Ref 20). The tremendous pressure and the high temperature generated by the process will "weld" the two active surfaces together. If the bonding energy of the "weld" is stronger than the cohesive energy of the workpiece materials, then workpiece adhesion may be formed on the tool (Ref 21). This is once more demonstrated in the case of friction drilling.

Figure 8(b) shows microstructure of the area in the bushing with the cross-section parallel to the plane of the sheet, marked as line F-F in Fig. 2(c). Compared with the white-etching layers seen in AISI 4130 steel in Fig. 6, Fig. 8(b) shows much less

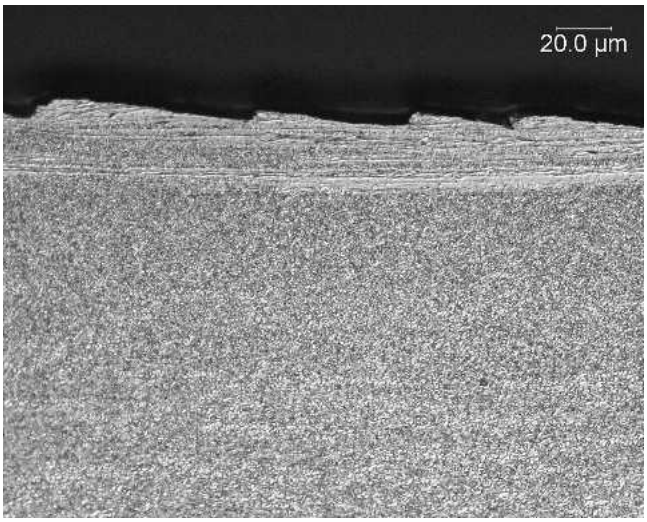

Fig. 6 Cross-sectional view of line D-D of the bushing of AISI 4130 in Fig. 2(b), microstructure of the near-hole area showing a row of overlapping zones of high strain (2% nital etchant)

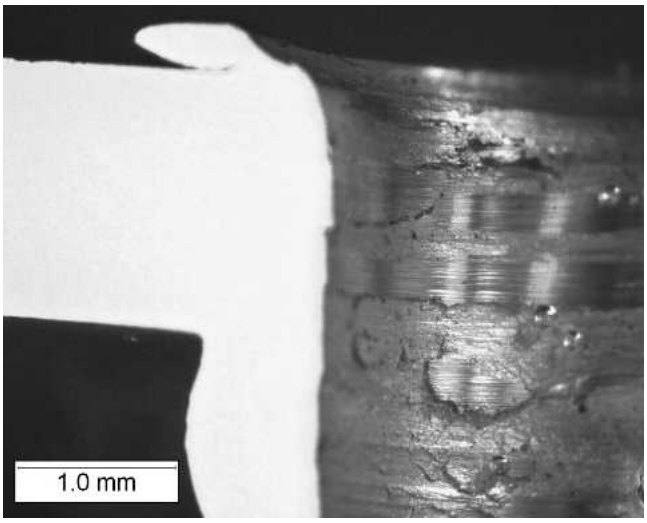

Fig. 7 Image of the inside of the hole in the Al 5052 sheet showing extensive plastic deformation, delamination, uplift, abrasion, and scored features

obvious development of a discontinuous zone of near-surface deformation adjacent to the bore surface.

3.3 CP Ti

CP titanium was the most difficult of the four materials to friction drill. The shape of the bushing in friction drilled CP titanium, as shown in Fig. 2(d), is short and thick, compared with bushings of other work-materials in Fig. 2. This is also evident in the quantitatively measured bushing height and diameter summarized in Table 3. It was necessary to reduce the tool rotational speed and introduce a commercial lubricant (Form Drill FD-KSO-2, Libertyville, IL) to enable the hole and bushing to be formed properly. Despite the use of reduced speeds and drilling lubricant, the internal surface of friction drilled CP titanium holes, as shown in Fig. 9, was damaged to an even greater extent than that of aluminum (Fig. 7). Close-up views of two areas along the hole, marked by boxes G and H in Fig. 2(d), are shown in Fig. 10(a) and 10(b), respectively. The wall consisted of either layers or localized pockets of severely deformed work-material.

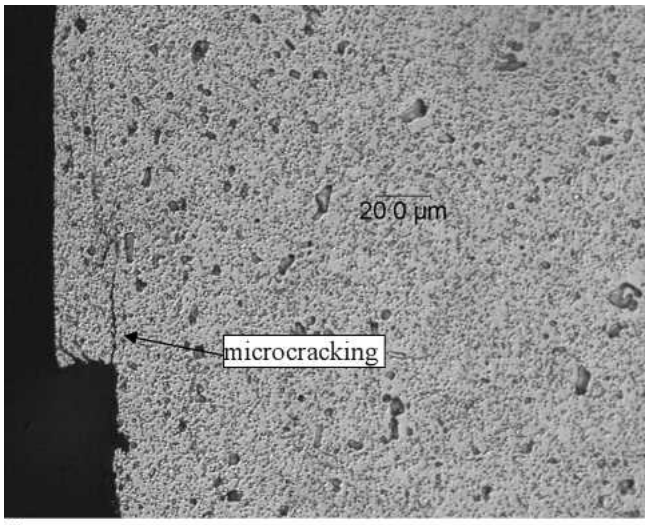

(a)

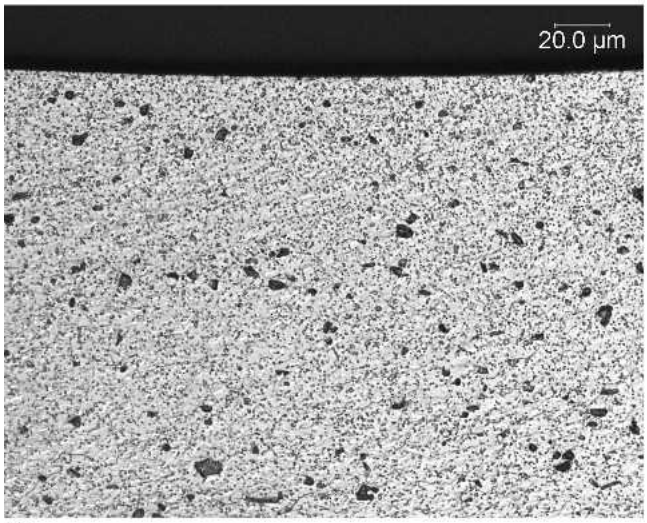

(b)

Fig. 8 (a) Close-up view of box E in Fig. 2(c), microstructure of Al 5052 showing a fine crack parallel to the hole wall above a region where a section of wall material was torn free, and (b) cross-sectional view of line F-F in Fig. 2(c), microstructure showing very subtle evidence for shear from right to left, but showing no clear boundary between highly-deformed material and the underlying grain structure (Keller's etch)

Figure 11 shows the cross-sectional view parallel to the titanium sheet, marked by line I-I in Fig. 2(d), of the friction drilled hole in the bushing. The flow of material from left to right and a cluster of cracks, marked by L and about 20 μm long, can be identified near the tip of the large crack of the torn surface layer (about 50 μm thick). This cluster of cracks is likely generated by the stress concentration at the interface of delaminating surface layers. Another cluster of very fine microcracks, marked by M and about 5-8 μm long, occurs at the interface between the deformed surface layer and the base material. These cracks could be induced possibly by thermal stress due to the high temperature gradient on the Ti surface layers during friction drilling.

Figure 12 compares the subsurface Knoop hardness versus depth profiles of the aluminum and titanium sheet. For titanium, the highly-deformed swirled regions, like those shown in Fig. 10 had Knoop microindentation hardness values ranging from about

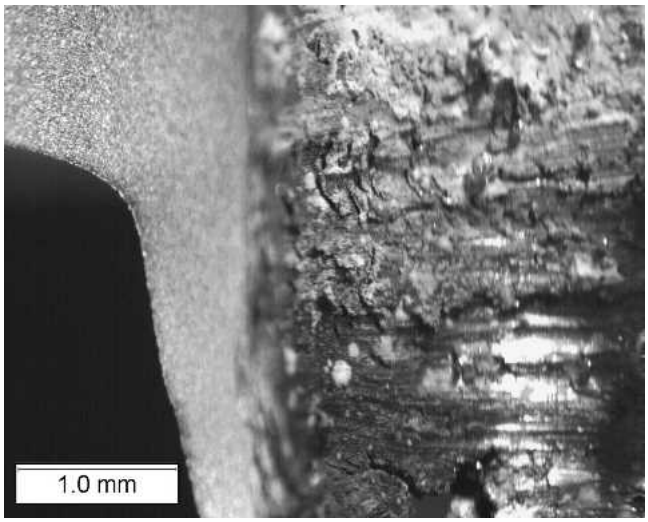

Fig. 9 Severe plastic deformation and tearing damage in the interior of the hole produced on friction-drilled CP Ti sheet

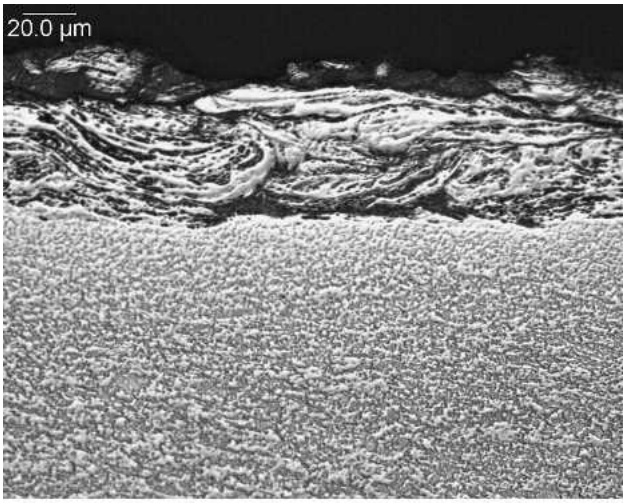

(a)

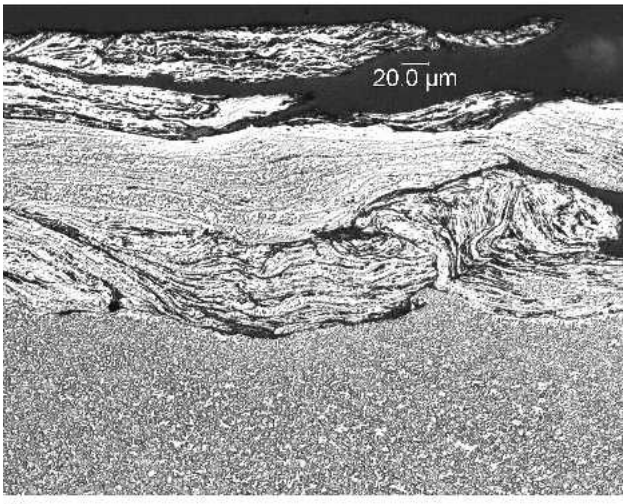

(b)

Fig. 10 Areas of intense shear and swirling of the Ti sheet material adjacent to the hole surface: (a) box G in Fig. 2(d) near the center of the hole length and (b) thicker overlapping layers of severe deformation near the exit end of the bushing in box H in Fig. 2(d)

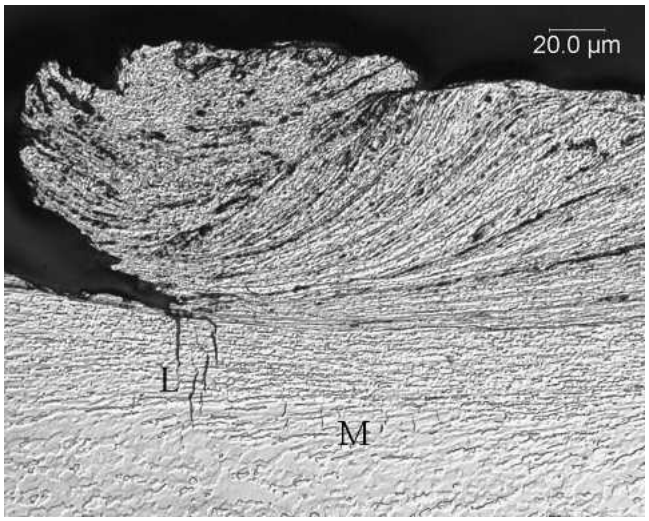

Fig. 11 Cross-sectional view of line I-I in Fig. 2(d), showing swirl of deformed Ti on the surface of the hole, cracks extending from the surface inward, and smaller cracks within the grains below the high-strain surface layers

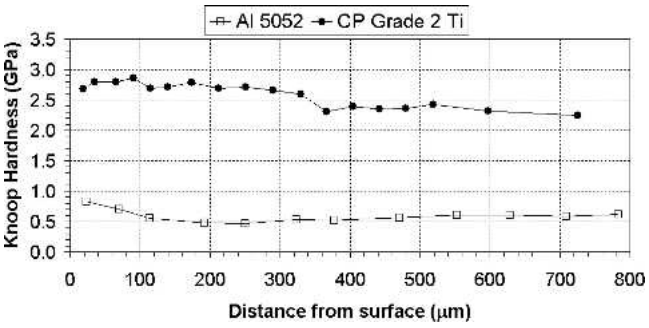

Fig. 12 Knoop microindentation subsurface hardness profile of the friction-drilled bore for Al 5052 and CP Ti (0.245 N force used)

2.6 to 3.5 GPa, while the granular regions just below the swirled region had hardness values of about 2.2 GPa. For aluminum, due to its high thermal conductivity, the reduction of hardness is gradual and deep (over 200 μm) into the workpiece.

4. Summary

Friction drilling of sheet metal results in a highly sheared microstructural condition in the vicinity of the hole bores and in the material extruded above and below the plane of the original sheet stock. The development of the microstructures described here is affected by the magnitude of the friction forces and heat produced during the friction drilling process. Depending on the thermal conductivity and frictional energy generated during drilling, this localized heating can reduce the magnitude of work hardening that would otherwise occur by deformation alone. Adherence of work-material to the tool breeds self-mated sliding conditions that tend to increase the frictional work done and thus the energy required to create a hole. The surface quality of holes is compromised by such conditions and may be a factor in reducing the fatigue life of joints made using this process unless less transfer-prone tooling and/or lubricants can be found.

The heat produced by friction drilling must be dissipated. Some heat goes into the tool, a portion transfers to the work-piece, and the rest is dissipated to the surroundings. There is no direct microstructural evidence for melting of work-material in friction drilling. It is entirely possible, even probable, however, that a very small amount of melting occurred at some thin surface regions.

Acknowledgments

A portion of this research was sponsored by the U.S. Department of Energy, Assistant Secretary for Energy Efficiency and Renewable Energy, Office of FreedomCAR and Vehicle Technologies, as part of the High Strength Weight Reduction Materials Program, under Contract No. DE-AC05-00OR22725 with UT-Battelle, LLC. Program management and guidance by Dr. Phil Sklad, is greatly appreciated, as was the assistance of Tom Geer, Oak Ridge National Laboratory, who prepared the metallographic specimens and worked to find suitable etchants to reveal the structures of interest.

References

1. J.A. van Geffen, Piercing Tools, US Patent No. 3 939 683, 1976
2. J.A. van Geffen, Method and Apparatuses for Forming by Frictional Heat and Pressure Holes Surrounded Each by a Boss in a Metal Plate or the Wall of a Metal Tube, US Patent No. 4 175 413, 1979
3. J.A. van Geffen, Rotatable Piercing Tools for Forming Holes Surrounded Each by a Boss in Metal Plates or the Wall of Metal Tubes, US Patent No. 4 177 659, 1979
4. J.A. van Geffen, Rotatable Piercing Tools for Forming Bossed Holes, US Patent No. 4 185 486, 1980
5. G.D. Head, W.C. Le Master, L.P. Bredesky, and D.C. Winter, Flow Drilling Process and Tool Therefore, US Patent No. 4 428 214, 1984
6. A.J. Hoogenboom, Flow Drill for the Provision of Holes in Sheet Material, US Patent No. 4 454 741, 1984
7. J.E. France, J.B. Davidson, and P.A. Kirby, Strength and Rotational Stiffness of Simple Connections to Tubular Columns Using Flowdrill Connectors, *J. Const. Steel Res.,* Vol 50, 1999, p 15-34
8. J.E. France, J.B. Davidson, and P.A. Kirby, Moment-Capacity and Rotational Stiffness of Endplate Connections to Concrete-filled Tubular Columns with Flowdrilled Connectors, *J. Const. Steel Res.,* Vol 50, 1999, p 35-48
9. J.E. France, J.B. Davidson, and P.A. Kirby, Strength and Rotational Response of Moment Connections to Tubular Columns Using Flowdrill Connectors, *J. Const. Steel Res.,* Vol 50, 1999, p 1-14
10. K. Overy, Flowdrilling—Bush Formation in Thin Metal, *Chartered Mech. Eng.,* Vol 25 (No. 7), 1978, p 70-71
11. D. Bak, Friction, Heat from Integral Bushings, *Design News,* Vol 43 (No. 11), 1987, p 124
12. M. Kerkhofs, M.V. Stappen, M. D'Olieslaeger, C. Quaeyhaegens, and L.M. Stals, The Performance of (Ti,Al)N-coated Flowdrills, *Surf. Coat. Technol.,* Vol 68/69, 1994, p 741-746
13. S.F. Miller, S.B. McSpadden, H. Wang, R. Li, and A.J. Shih, Experimental and Numerical Analysis of the Friction Drilling Process, ASME, Journal of Manufacturing Science and Engineering (submitted)
14. Y.S. Touloukian, R.W. Powell, C.Y. Ho, and P.G. Klemens, Thermal Conductivity: Metallic Elements and Alloys, *Thermophysical Properties of Matter,* Vol 1, IFI/Plenum Data Corp., New York, NY, 1970
15. Y.S. Touloukian and E.H. Buyco, Specific Heat: Metallic Elements and Alloys, *Thermophysical Properties of Matter,* Vol 4, IFI/Plenum Data Corp., New York, NY, 1970
16. E.A. Avallone and T. Baumeister III, *Marks' Standard Handbook for Mechanical Engineers,* 9th ed., McGraw-Hill Book Company, 1987
17. S. Hoyt, Metals Properties, *ASME Handbook,* 1st ed., McGraw-Hill Book Company, New York, NY, 1954
18. *Metals Handbook, Desk Edition,* 2nd Ed., ASM International, 1998
19. Atlas of Microstructures of Industrial Alloys, *Metals Handbook,* 8th ed., Vol 7, ASM International, 1972, p 341-342
20. N. Sato, O. Terada, and H. Suzuki, Adhesion of Aluminum to WC-Co Cemented Carbide Tools, *J. Jpn. Soc. Powder Powder Metall.,* Vol 44 (No. 4), 1997, p 365-368
21. Y. Li, T.L. Ngai, W. Xia, Y. Long, and D. Zhang, A Study of Aluminum Bronze Adhesion on Tools during Turning, *J. Mater. Proc. Technol.,* Vol 138, 2003, p 479-483